Local Structure-based Region-of-Interest Retrieval in Brain MR Images

Devrim Unay*, Ahmet Ekin, and Radu Jasinschi

***Abstract*—The aging population and the growing amount of medical data have increased the need for automated tools in the neurology departments. Although the researchers have been developing computerized methods to help the medical expert, these efforts have primarily emphasized improving the effectiveness in single patient data, such as finding a brain lesion and computing its size. However, patient-to-patient comparison that should help improve diagnosis and therapy has not received as much attention. To this effect, this paper introduces a fast and robust region-of-interest retrieval method for brain magnetic resonance (MR) images. We make several contributions to the domains of brain MR image analysis, and search and retrieval: 1)We show the potential and robustness of local structure information in the search and retrieval of brain MR images. 2)We provide analysis of two complementary features, local binary patterns and Kanade-Lucas-Tomasi feature points, and their comparison with a baseline method. 3)We show that incorporating spatial context in the features substantially improves accuracy. 4)We propose to automatically extract dominant local binary patterns and demonstrate that using dominant features improves retrieval relative to the conventional local binary pattern approach. Comprehensive experiments on real and simulated datasets revealed that dominant local binary patterns with spatial context is robust to geometric deformations and intensity variations and have high accuracy and speed. The proposed method can not only aid the medical expert in disease diagnosis, or be used in scout (localizer) scans for optimization of acquisition parameters, but also support low power devices that we believe will find increasing usage in hospitals.**

***Index Terms*—Brain MR image retrieval, local structure analysis, local binary patterns, Kanade-Lucas-Tomasi feature points, spatial descriptors, medical databases, neurodegenerative diseases.**

I. Introduction

THE advances in the medical imaging technology allow for in-vivo visualization and analysis of human body with unprecedented accuracy and resolution. A diagnosis by a specialist often requires a visit to a radiology department to obtain various images that highlight the suspected pathology. Despite the high resolution of the acquired images, image-based diagnosis often utilizes a considerable amount of qualitative measures. To improve the diagnosis and efficiency, the research in medical image analysis has focused on the computation of quantitative measures by automating some of the error-prone and excruciatingly time-consuming tasks, such as segmentation of a structure.

This work was supported in part by the Marie Curie Programme of the European Commission under FP6 IRonDB project MTKI-CT-2006-042717.

D. Unay, A. Ekin, and R. Jasinschi are with the Video Processing and Analysis Group, Philips Research Europe, 5656 AE Eindhoven, The Netherlands (devrim.unay@philips.com, ahmet.ekin@philips.com, radu.jasinschi@philips.com).

A less emphasized approach for improving diagnosis has been comparison of multiple patients, their pathologies, and progresses by search and retrieval systems. This should especially improve the diagnosis of diseases whose causes and progress have not yet been completely unraveled, and diseases that affect large number of patients. The area of neurology can greatly benefit from such a methodology because the diagnosis of neurodegenerative diseases from one patient data has limitations (A review of 13 neuropathologically confirmed studies show that a clinical diagnosis of Alzheimer's Disease has an average sensitivity of 81% and specificity of 70% [1]). Accordingly, this paper focuses on region-of-interest retrieval of unregistered brain MR images although the presented methods should be applicable to other organs. In particular, we would like to find similar slices in an unregistered brain MR database given a query slice, automation of which can aid the medical expert in diagnosis of structure-specific diseases, such as hippocampus or basal ganglia disorders.

In the medical domain, to obtain clinically useful images imaging system operators typically acquire scout (localizer) and target scans, where the former is visually examined to specify acquisition parameters for the latter. Hence, the presented methods can also be used to automate the examination of the scout images to set parameters for the target scan.

The extensive research on search and retrieval in the domain of multimedia confirms the challenging nature of this problem [2]-[3]. In the domain of medical data, there are domain or even modality-specific differences and challenges. The captured images are usually single channel (gray-scale) that differs from multi-channel (e.g. RGB) nature of consumer image and video data. In some medical modalities, such as CT (Computed Tomography) and X-ray, intensity has an absolute scale. In MR, they vary with the scanning parameters, but also with the age of the device and the patient characteristics. To aggravate the problem, the intensity values of a specific tissue may also be non-stationary within a single MR image (a fact known as intensity non-uniformity or bias field) because of imperfect magnetic field and patient-dependent local perturbations. Furthermore, the characteristics of relevant and irrelevant segments of the data are very close to each other for the databases that are specific to a modality and an organ, such as brain MR database.

To the best of our knowledge, only Bucci et al. [4] consider a similar search and retrieval problem as ours, that is, retrieving the relevant slice from a brain MR image sequence in response to a given sample slice. Their method performs retrieval of the relevant slice using Principal Component Analysis (or the so-called eigenimages), but requires a com-

putationally expensive registration and intensity normalization step beforehand.

Others working on the search and retrieval of MR images mainly focused on the shape information: Hsu et al. [5] introduced a method based on the shape of the brain ventricles. Robinson et al. [6] and Petrakis and Faloutsos [7], both proposed shape based retrieval methods that require manual delineation of the anatomical structures in question. More recently, Huang et al. [8] used geometric features and Fourier descriptors to represent brain images of pediatric patients, but required registered images.

In CT, because intensity has an absolute scale, many systems have exploited it together with image structure and shape information in feature extraction, e.g., by using histogram, moment invariants and co-occurrence matrix representations in combination [9], [10]. Traina et al. [11] introduced a structure-based retrieval solution for human brain images by using wavelets. Ghebraeb et al. [12] focused on shape information and proposed to use contour curvatures of expert delineated vertebrae in X-ray images. Retrieval of medical images from multiple modalities is challenging due to the presence of image related problems specific to different modalities. The system in [13] uses co-occurrence matrix representations to achieve retrieval of CT and MR images of different tissues, while the one in [14] employs color quantization and wavelet responses to retrieve images of different body parts acquired with various modalities. Other medical modalities, such as positron emission tomography [15], have been less investigated [16].

The rest of the paper is organized as follows: Section II provides an insight into the approach used in this work as well as our contributions. Section III details the pre-processing applied to the images. Sections IV and V present the feature extraction and description stages of our solution, where four local structure-based methods and one edge-related baseline method are introduced. Section VI explains how the retrieval is performed. Experimental data and results are presented in Section VII. Finally, the conclusions and the related future works are given in Section VIII.

II. Our Approach and Contributions

In this paper, we focus on a retrieval problem where the most similar slices to the given query slice are searched. The challenges for this problem include:

- MR intensity variations from one patient to another because of possible differences in MR settings. This limits the use of intensity information in comparing different datasets.
- Intensity variations within the same dataset (intensity non-uniformity or bias field) due to imperfect, inhomogeneous magnetic field. This requires the use of computational bias field correction algorithms.
- The high similarity between irrelevant and relevant segments in medical images makes their search and retrieval more challenging.
- Inter and intra-patient misalignment of images, because of which anatomical structures are observed at different spatial positions, orientations and scales in the images. Although registration could solve this problem, it is too computational and impractical for low power mobile devices or for the scouting application where fast image acquisition is crucial for the clinical centers.
- Abnormalities of brain structure, such as ventricular enlargement or cerebral atrophy, tumors.

To solve the above problems, this paper introduces the following contributions:

- We introduce a fast and robust search and retrieval method of brain MR images. Not only the retrieval performance is invariant to some basic geometric transformations and intensity variations, but also the system avoids the computationally intensive registration, intensity normalization, and bias field correction steps.
- We propose to use local structure features instead of intensities, because intensity is non-standard and sensitive to MR imaging artifacts. The local structure features are robust to both inter- and intra-scan intensity variations.
- We show the search and retrieval effectiveness of two local structure features: 1) local binary patterns (LBP) proposed by Ojala et al. [17], and 2) Kanade-Lucas-Tomasi (KLT) feature points. The choice of the two is not arbitrary. LBP operates locally and treats every local region equally. On the contrary, KLT selects the predefined number of features that are the most salient.
- To remedy the high feature space similarity of relevant and irrelevant segments, we use a context-based description of features. The spatial description of features increases the retrieval performance significantly and provides robustness to large abnormalities seen in severe cases.
- We show that using only the most dominant local binary patterns in the query improves retrieval accuracy while reducing dimensionality of the data.

III. Pre-Processing

A typical MR image of the head consists of brain tissue as well as background and non-brain structures, like skull and skin in which we are not interested. Hence, we perform the extraction of the brain tissue by using the Brain Extraction Tool (BET) [18].

Moreover, as misalignment of images is a common problem in magnetic resonance imaging, we benefit from a mid-sagittal plane detection algorithm [19] that indicates orientation, in order to compensate for rotation in spatial description of the features, which will be explained afterwards.

IV. Structure-based Feature Extraction

In this section, we first describe LBP, a computationally very efficient method to extract local structure and due to its local nature invariant to bias field [20]. Afterwards, we describe KLT feature points that correspond to the most salient local regions of the image.

A. Local Binary Patterns

Recently, Ojala et al. [17] introduced LBP, which is a grayscale invariant local texture descriptor with low computational complexity. Subsequent studies have shown that LBP is

promising in the computer vision field, including industrial inspection [21], motion analysis [22], and face recognition [23]. However, its application in the medical field has been mainly limited to adenoma detection in endoscopic images [24] and plaque segmentation in ultrasound images [25].

LBP operator ($LBP_{P,R}$) describes the local structure pattern by thresholding a neighborhood with the gray value of its center pixel (g_c) and represents the result as a binary code. The neighborhood is formed by a symmetric neighbor set of P pixels $g_p(p = 0, \ldots, P-1)$ on a circle of radius R.

$$LBP_{P,R} = \sum_{p=0}^{P-1} s(g_p - g_c)2^p, \qquad s(x) = \begin{cases} 1, & x \geq 0 \\ 0, & x < 0 \end{cases} \tag{1}$$

Extended versions of the original operator are introduced in [17] as (1) $LBP^{ri}_{P,R}$: rotation invariant, (2) $LBP^{u2}_{P,R}$: uniform, and (3) $LBP^{riu2}_{P,R}$: rotation invariant and uniform operators.These extensions provide not only robustness of patterns to noise and rotation, but also dimensionality reduction in the pattern space, e.g., structure in a 3×3 neighborhood is represented by 256, 36, 59, and 10 different patterns using $LBP_{8,1}$, $LBP^{ri}_{8,1}$, $LBP^{u2}_{8,1}$, and $LBP^{riu2}_{8,1}$ operators, respectively.

B. KLT Feature Points

LBP computes structure features in all local regions of the image. However, one may argue that not all parts of an image contain valuable information. Consequently, researchers proposed to find interesting regions of an image using detectors, such as the SIFT descriptor [26]. Another exemplary work is the KLT feature tracker [27], [28], which focuses on the regions (so-called *good features*) that can be tracked well. KLT method has been applied to various problems, such as registration in augmented reality systems [29], pedestrian tracking [30], and gestures and facial expressions tracking [31], but to the best of our knowledge its application in medical field is not yet realized.

Feature point selection in KLT is performed by searching the whole image through a window, and selecting the regions that have adequate intensity variation in vertical and horizontal directions, indicating they contain corner. Considering the local intensity variation matrix

$$Z = \begin{bmatrix} g_x^2 & g_x g_y \\ g_x g_y & g_y^2 \end{bmatrix} \tag{2}$$

where g_x and g_y are the partial derivatives of an input image $I(x, y)$, a region is accepted as a candidate feature point if both eigenvalues, λ_1 and λ_2, of Z exceed a predefined threshold, $min(\lambda_1, \lambda_2) > \lambda$. Consequently, the candidate feature points of the input image are ranked according to their strength defined by $min(\lambda_1, \lambda_2)$, and NF strongest ones are selected, with NF being the user-defined maximum number of features to be selected.

V. Feature Description

In this section we propose four methods based on either LBP or KLT features, and a baseline method for comparison.

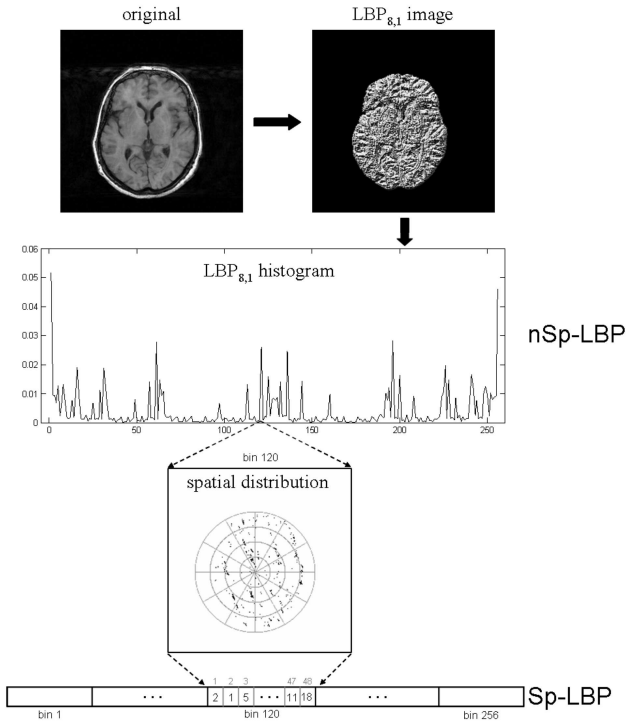

Fig. 1. Computation of LBP features.

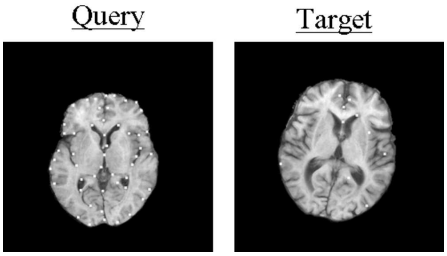

Fig. 2. A visual example of feature point matching. Among the 50 feature points (overlaid as white dots on the images) extracted from a query, 10 are matched on the target.

These five methods are organized depending on whether their features are described spatially (Sp) or not (nSp).

A. Non-Spatial Feature Description

nSp-LBP As LBP features correspond to all local regions of an image, we describe them by their statistical distribution. Therefore, in nSp-LBP we use the histogram of the extracted LBP image (Figure 1).

nSp-KLT Salient feature points extracted from an image will be successfully matched (and therefore preserved) on another if the two images are similar. Hence, nSp-KLT method extracts feature points from the query and attempts in matching them on the target (Figure 2). The number of matched feature points are then used as attributes in retrieval.

B. Spatial Feature Description

Sp-LBP This method exploits spatial indexing [32] of the LBP image histogram, where the entries of each

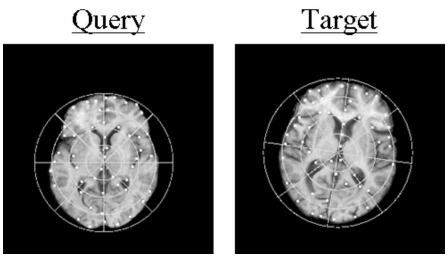

Fig. 3. Spatial distribution of 50 feature points extracted from a query and a target image. The grid is composed of 4 annular and 8 angular regions.

bin are spatially indexed over an annularly and/or angularly partitioned area (grid), as illustrated in Fig. 1. The grid used for spatial indexing is fitted on the largest brain area observed in an MR scan (image volume) providing a single reference for all the corresponding slices. Please note that, as the grid conforms to the largest brain area in each individual scan and is rotated relative to the corresponding mid-sagittal plane (detected in pre-processing), it serves as a scale, translation, and rotation invariant reference frame.

Sp-KLT This method skips the matching step in nSp-KLT and compares spatial distributions of feature points extracted from the query and the target simultaneously over a grid similar to the one used in the Sp-LBP method (Fig. 3).

Sp-Sobel As a baseline method, we use spatial indexing of edge points computed by Sobel operator.

VI. Retrieval

The aforementioned retrieval problem tackled in this work is to find the target slice from an MR scan that is the most similar to a query. Fig. 4 illustrates the retrieval scheme used for all five methods, where pre-processing and feature extraction/description steps have been previously explained. The measure of similarity between query and target brain slices is defined in two ways:

1)

$$D_1\left(p_q, p_t\right) = 1 - \sqrt{\sum_{\forall i}\left(p_q(i) - p_t(i)\right)^2} \qquad (3)$$

where p_q and p_t are the normalized histograms (features) of query and target, respectively. This measure is used with nSp-LBP, Sp-LBP, Sp-KLT, and Sp-Sobel methods.

2)

$$D_2 = \frac{\text{number of matched feature points}}{\text{number of feature points}} \qquad (4)$$

which is used with nSp-KLT method.

Both measures provide a *similarity score* in the range of [0-1], with scores closer to 1 indicating high-level of similarity between slices. Consequently, for a retrieval task the target slice with the highest score is assigned as the most similar one to the query and retrieved at rank=1.

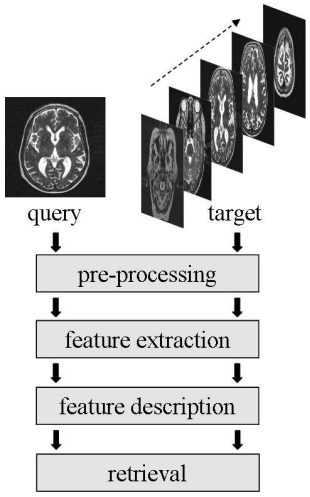

Fig. 4. Illustration of the retrieval scheme.

VII. Experimental Results

A. Image Data

The database used in this study consists of T1-weighted axial brain MR scans from 15 subjects with 50 slices per scan. Their acquisition is performed on a Philips Intera 1.5T whole body scanner at Leiden University Medical Center by using spin echo weighted images (TR/TE: 25,6/12 ms, FLIP: 45) with 250mm FOV, 3mm slice thickness, no slice gap and 256x256 matrix.

We acknowledge that our database size, which is typical of medical domain, is small relative to those in computer vision studies. However because the retrieval task in this study is defined as searching for a key-slice within a single MR scan, scalability of retrieval is constrained by the number of slices in the scans and not by the number of scans in the database, and therefore we believe that our solution will be equally applicable to larger datasets.

Changes in cerebral ventricles and the surrounding structures are often associated with central nervous system disorders. Accordingly, from each patient's brain MR scan in our database we manually selected the following four slices (landmarks), which are related to the cerebral ventricles:

- Landmark #1 (L1) is associated with the fourth ventricle.
- Landmark #2 (L2) discloses the ventricular triangle.
- Landmark #3 (L3) is the slice where lateral ventricles merge to form a butterfly shape.
- Landmark #4 (L4) corresponds to the first slice, in the direction from the feet to the head, where the ventricles are not observed anymore.

An example of the landmarks selected from two patients' scans is displayed in Fig. 5, where one can notice that brain structures are not necessarily observed at the same slice level.

Additionally, three simulated bias fields from the BrainWeb MR Simulator [33] are utilized to test robustness of retrieval with respect to intensity variations (Fig. 6). These bias fields provide smooth variations of intensity across the image. Based on the conventional assumption that the bias field is multiplicative, original images are first corrected by the N3 method of

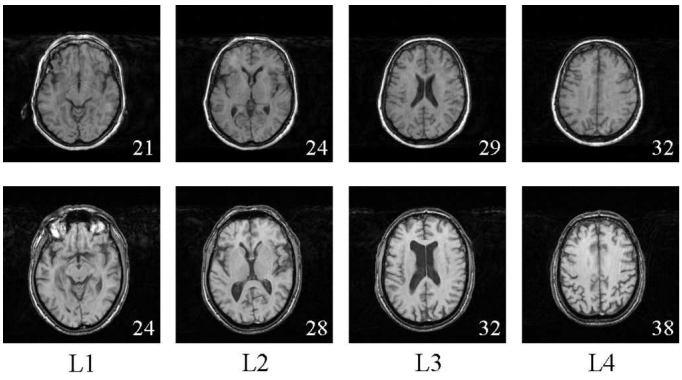

Fig. 5. Examples of landmark slices manually selected from the MRI scans of two patients displayed in each row with the corresponding slice numbers.

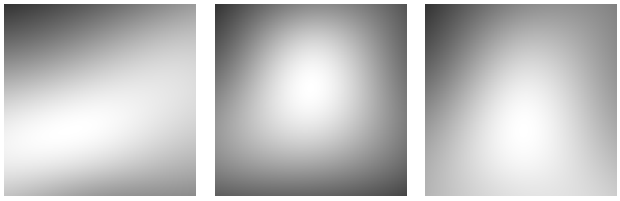

(a) A (b) B (c) C

Fig. 6. Examples of simulated bias fields used in this study. Intensity variations are exaggerated for visual purposes.

Sled et al. [34], and then degraded by multiplying with the bias fields.

B. Performance of Retrieval

Performance of image retrieval systems is generally measured by $precision = \frac{\#\ relevant\ returns}{\#\ returns}$ and $recall = \frac{\#\ relevant\ returns}{\#\ relevant\ items}$. They are not descriptive enough for our problem, because the number of relevant items per retrieval is restricted to one. Therefore, we measure error of a retrieval task as the sum actual distances of returns ranked higher than the relevant slice:

$$error = \sum_{i=1}^{N-1} (S_i - S_N) \times d \tag{5}$$

where N is the rank of the relevant slice, S_i the slice number at rank=i, and d the slice thickness. As our database consists of 15 MR scans with 4 landmark slices per scan, there are 15×4 query landmarks. Excluding the retrieval tasks where query and target originate from the same scan, there are $15 \times 4 \times 14 = 840$ unique retrieval tasks in total. Accordingly, performance of retrieval in the following results is measured as the average error of all unique retrieval tasks, as well as the average rank of the corresponding relevant slices.

Table I presents retrieval performances achieved using nSp-LBP, where - among various combinations of different LBP operators - only the best results are displayed. We observe that combinations of different LBP operators produce more accurate results most probably due to various scales covered by individual operators.

Table II displays performance of Sp-LBP (using a grid with 12 angular and 4 annular splits) for various $LBP_{8,1}$ operators.

TABLE I
PERFORMANCES OF NSP-LBP RETRIEVAL

Operator	Error [mm] - Rank
$LBP_{8,1}$	188.6 - 9.3
$LBP_{8,1} + LBP^{u2}_{16,2}$	165.7 - 8.5
$LBP_{8,1} + LBP^{u2}_{16,2} + LBP^{u2}_{24,3}$	131.3 - 7.3

Performances of retrieval using nSp-LBP.

TABLE II
PERFORMANCES OF SP-LBP RETRIEVAL

Operator	Error [mm] - Rank	Error [mm] - Rank (DP^a ratio)
$LBP_{8,1}$	33.1 - 3.6	29.3 - 3.4 (0.6)
$LBP^{ri}_{8,1}$	50.5 - 4.7	49.5 - 4.7 (0.6)
$LBP^{u2}_{8,1}$	34.2 - 3.8	34.0 - 3.8 (0.9)
$LBP^{riu2}_{8,1}$	44.6 - 4.4	44.1 - 4.4 (0.4)

Performances of retrieval using Sp-LBP with all patterns (2^{nd} column) and dominant patterns (3^{rd} column).
^{a}Dominant Patterns

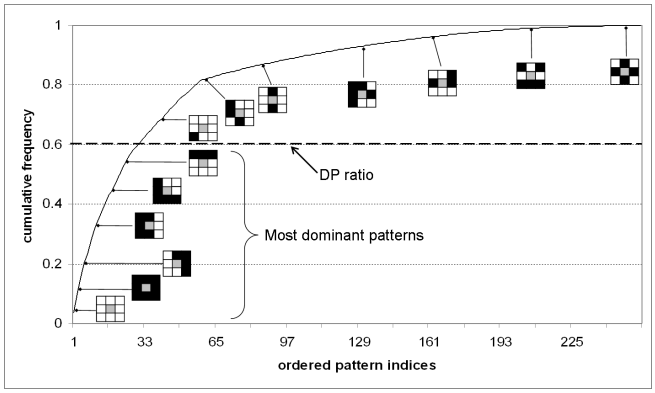

Fig. 7. Cumulative frequency plot of $LBP_{8,1}$ patterns.

Initial tests are done using all features (patterns), where we observe that addition of spatial information highly improves the retrieval performance. Conventional LBP ($LBP_{8,1}$) outperforms its rotation invariant and/or uniform counterparts due to its higher number of features. In order to observe the effect of feature selection on retrieval performance, the same test is repeated using only the most dominant patterns observed in the query. Suppose that a cumulative distribution is constructed from the ordered pattern occurrences as in Fig. 7, then a pattern is said to be dominant if it belongs to the top portion of this distribution set by a user-defined threshold (DP ratio). Accordingly, altering the DP ratio will result in different number of dominant patterns to be selected. Corresponding results in Table II show the best retrieval performances achieved by dominant patterns, where we observe that feature selection further improves retrieval.

Performance of nSp-KLT method depends on the optimization of different parameters affecting the feature point extraction and matching steps (e.g. number of features, search window size). Table III unveils an exponential decay in the retrieval error and rank with the number of features. Further tests revealed that higher number of features and/or larger search window produce more accurate result with exponen-

TABLE III
PERFORMANCES OF NSP-KLT RETRIEVAL

NF[a]	Error [mm] - Rank
50	95.7 - 6.3
100	61.3 - 5.0
150	47.9 - 4.3
200	44.2 - 4.3

Performances of retrieval using nSp-KLT.
[a]Number of features

TABLE IV
PERFORMANCES OF SP-KLT RETRIEVAL

AS[a]	AnnS[b]	Error [mm] - Rank
4	2	143.8 - 8.4
8	3	117.2 - 7.5
12	4	81.9 - 6.3

Retrieval performance of Sp-KLT.
[a]angular split, [b]annular split

tial increase in computational expense, therefore number of features=150 and search window size=7 are used in the tests hereafter.

Sp-KLT avoids matching of feature points and focuses on their spatial distribution over a tessellated grid (through annular and angular splits). Table IV displays the retrieval results of Sp-KLT with respect to varying tessellations, where we observe a positive relation between the retrieval performance and the number of tessellations. Notice that, Sp-KLT results in considerably lower performances relative to those of nSp-KLT (see Table III) due to the avoided feature point matching step.

Finally, retrieval error of the Sp-Sobel method, over a grid with 12 angular and 4 annular splits, is measured as 53.8 mm with the average rank of relevant slice being 5.0.

In addition, performance analysis for individual landmarks revealed that all five methods encountered more difficulty in retrieving outermost landmarks (L1 and L4), probably because similarity in brain tissue between these landmarks and their neighboring slices is higher.

Influence of Geometric Deformations: In this part, retrieval performances of the three promising methods (Sp-LBP, nSp-KLT, and Sp-Sobel) are tested in the presence of geometric deformations (rotation and scale) and bias field. As rotation higher than 15° is not realistic in brain MR images, we rotated the database in the axial plane by ± 15 degrees and repeated the retrieval using the original images as query and rotated versions as target. The results showed that Sp-LBP and nSp-KLT are robust to rotation, while the performance of Sp-Sobel considerably decreased.

Effect of scaling on the retrieval performances of the methods can be seen in Table V, where we observe that Sp-LBP is robust at scales above 0.7, while nSp-KLT copes better and Sp-Sobel copes worse with scaling. Relatively low errors achieved by nSp-KLT at scales of 0.9 to 0.7 can be associated with varying saliency of feature points at different scales.

Influence of Bias Field: Effect of several bias fields (Figure 6) with different intensity variations on retrieval performance of the methods is also tested. Table VI displays the results for the bias fields at 40% intensity variation. We observe that addition of bias field has slight effect on the performances.

TABLE V
EFFECT OF SCALING ON RETRIEVAL ERRORS

	Scaling Factor					
method	1.0	0.9	0.8	0.7	0.6	0.5
Sp-LBP[a]	29.3	31.4	30.1	37.2	38.5	38.0
nSp-KLT[b]	47.9	42.6	41.7	40.6	46.0	72.0
Sp-Sobel[c]	53.8	52.2	78.1	82.0	59.3	63.4

Retrieval errors [mm] of Sp-LBP, nSp-KLT, and Sp-Sobel relative to scaling.
[a]$LBP_{8,1}$ with DP ratio=0.6, angular split=12, annular split=4.
[b]Search window size=7, number of features=150.
[c]Angular split=12, annular split=4.

TABLE VI
EFFECT OF BIAS FIELD ON RETRIEVAL ERRORS

		Bias Field		
method	original	A	B	C
Sp-LBP[a]	29.3	29.8	29.7	31.0
nSp-KLT[b]	47.9	48.4	47.2	47.2
Sp-Sobel[c]	53.8	57.9	55.3	51.9

Retrieval errors [mm] of Sp-LBP, nSp-KLT, and Sp-Sobel relative to bias field.
[a]$LBP_{8,1}$ with DP ratio=0.6, angular split=12, annular split=4.
[b]Search window size=7, number of features=150.
[c]Angular split=12, annular split=4.

In consequence of our observations so far, we recommend the use of Sp-LBP with dominant patterns for search and retrieval of a key-slice from an image volume, because nSp-KLT is computationally inefficient due to the feature point matching step.

C. Computational Complexity

Algorithms used in this work are all implemented in C/C++ and the average processing time per slice (excluding the preprocessing step) on an Intel Pentium processor (2.8 GHz) with 1G memory is measured as 103ms for Sp-KLT, 201ms for nSp-KLT, and around 50ms for the rest. Please note that, computation time can be further reduced using database indexing, optimized software, and dedicated hardware.

VIII. CONCLUSION AND FUTURE WORK

In this paper, we presented a novel and fast region-of-interest retrieval system for brain MR images where the task is to search for a key-slice from an image volume. Considering the intensity-related problems present in MR we tested two complementary intensity invariant structure features, local binary patterns and Kanade-Lucas-Tomasi feature points. Comparison of the two with a baseline method provided us with useful insights and trade-offs. We performed comprehensive experiments on real and simulated data and showed that incorporating spatial information in the local binary patterns substantially improved accuracy, whereas avoiding matching of Kanade-Lucas-Tomasi feature points considerably degraded performance. The experiments further revealed that dominant local binary patterns with spatial context consistently outperformed its rivals in retrieval accuracy and it is observed to

be robust to common anomalies, such as abnormal cerebral ventricles, present in the data. Moreover, this retrieval method is observed robust to bias fields at 40% intensity variation, rotation up to $\pm 15^{\circ}$, and downsizing at scales above 0.7. In conclusion, the proposed retrieval method is fast and robust, has high accuracy, and does not require registration, intensity normalization or bias field correction.

The retrieval problem addressed in this study has an inherent difficulty due to the very similar content present in the data, and therefore there is room for improvement. We believe that incorporating multiresolution analysis and shape information into the proposed method may improve its accuracy.

ACKNOWLEDGMENT

The authors thank Prof. Mark van Buchem and Dr. Jeroen van der Grond from the Department of Radiology, Leiden University Medical Center for the discussions and data support.

REFERENCES

[1] D. S. Knopman, S. T. DeKosky, J. L. Cummings, H. Chui, J. Corey-Bloom, N. Relkin, G. W. Small, B. Miller, and J. C. Stevens, "Practice parameter: Diagnosis of dementia (an evidence-based review): Report of the Quality Standards Subcommittee of the American Academy of Neurology," *Neurology*, vol. 56, no. 9, pp. 1143–1153, 2001. [Online]. Available: http://www.neurology.org/cgi/content/abstract/56/9/1143

[2] Y. Rui, T. Huang, and S. Chang, "Image retrieval: current techniques, promising directions and open issues," *Journal of Visual Communication and Image Representation*, vol. 10, no. 4, pp. 39–62, Apr. 1999.

[3] M. S. Lew, N. Sebe, C. Djerba, and R. Jain, "Content-based multimedia information retrieval: state of the art and challenges," *ACM Transactions on Multimedia Computing, Communications, and Applications*, vol. 2, no. 1, pp. 1–19, Feb. 2006.

[4] G. Bucci, S. Cagnoni, and R. D. Domenicis, "Integrating content-based retrieval in a medical image reference database," *Computerized Medical Imaging and Graphics*, vol. 20, no. 4, pp. 231–241, 1996.

[5] C.-C. Hsu, W. W. Chu, and R. K. Taira, "A knowledge-based approach for retrieving images by content," *IEEE Transactions on Knowledge and Data Engineering*, vol. 8, no. 4, pp. 522–532, 1996.

[6] G. P. Robinson, H. D. Tagare, J. S. Duncan, and C. C. Jaffe, "Medical image collection indexing: shape-based retrieval using kd-trees," *Computerized Medical Imaging and Graphics*, vol. 20, no. 4, pp. 209–217, 1996.

[7] E. G. M. Petrakis and C. Faloutsos, "Similarity searching in medical image databases," *IEEE Transactions on Knowledge and Data Engineering*, vol. 9, no. 3, pp. 435–447, 1997.

[8] H. K. Huang, J. F. Nielsen, M. D. Nelson, and L. Lui, "Image-matching as a medical diagnostic support (DST) for brain diseases in children," *Computerized Medical Imaging and Graphics*, vol. 29, no. 2-3, pp. 195–202, 2005.

[9] A. Kak and C. Pavlopoulou, "Content-based image retrieval from large medical databases," in *1st International Symposium on 3D Data Processing Visualization and Transmission*, Padova, Italy, 2002, pp. 138–147.

[10] S.-N. Yu, C.-T. Chiang, and C.-C. Hsieh, "A three-object model for the similarity searches of chest CT images," *Computerized Medical Imaging and Graphics*, vol. 29, no. 8, pp. 617–630, 2005.

[11] A. J. M. Traina, C. A. B. Castañón, and C. Traina Jr., "Multiwavemed: a system for medical image retrieval through wavelets transformations," in *16th IEEE Symposium on Computer-Based Medical Systems*, New York, USA, 2003, pp. 150–155.

[12] S. Ghebraeb, C. C. Jaffe, and A. W. M. Smeulders, "Population-based incremental interactive concept learning for image retrieval by stochastic string segmentations," *IEEE Transactions on Medical Imaging*, vol. 23, no. 6, pp. 676–689, Jun. 2004.

[13] J. C. Felipe, A. J. M. Traina, and C. Traina Jr., "Retrieval by content of medical images using texture for tissue identification," in *16th IEEE Symposium on Computer-Based Medical Systems*, New York, USA, 2003, pp. 175–180.

[14] H. Müller, A. Rosset, J.-P. Vallét, and A. Geisbuhler, "Comparing feature sets for content-based image retrieval in a medical case database," in *Proceedings of SPIE Medical Imaging: PACS and Imaging Informatics*, San Diego, USA, 2004, pp. 99–109.

[15] J. Kim, W. Cai, D. Feng, and H. Wu, "A new way for multidimensional medical data management: volume of interest (VOI)-based retrieval of medical images with visual and functional features," *IEEE Transactions on Information Technology in Biomedicine*, vol. 10, no. 3, pp. 598–607, Jul. 1997.

[16] H. Müller, N. Michoux, D. Bandon, and A. Geisbuhler, "A review of content-based image retrieval systems in medical applications - clinical benefits and future directions," *International Journal of Medical Informatics*, vol. 73, no. 1, pp. 1–23, Feb. 2004.

[17] T. Ojala, M. Piettikäinen, and T. Mäenpää, "Multiresolution gray-scale and rotation invariant texture classification with local binary patterns," *IEEE Transactions on Pattern Analysis and Machine Intelligence*, vol. 24, no. 7, pp. 971–987, Jul. 2002.

[18] S. M. Smith, "Fast robust automated brain extraction," *Human Brain Mapping*, vol. 17, no. 3, pp. 143–155, Nov. 2002.

[19] A. Ekin, "Feature-based brain mid-sagittal plane detection by RANSAC," in *Proceedings of 14th European Signal Processing Conference*, Florence, Italy, 2006.

[20] D. Unay, A. Ekin, M. Cetin, R. Jasinschi, and A. Ercil, "Robustness of local binary patterns in brain MR image analysis," in *29th Annual International Conference of the IEEE-EMBS*, Lyon, France, 2007, pp. 2098–2101.

[21] T. Mäenpää, M. Turtinen, and M. Piettikäinen, "Real-time surface inspection by texture," *Real-Time Imaging*, vol. 9, no. 5, pp. 289–296, Oct. 2003.

[22] M. Heikkilä and M. Piettikäinen, "A texture-based method for modeling the background and detecting moving objects," *IEEE Transactions on Pattern Analysis and Machine Intelligence*, vol. 28, no. 4, pp. 657–662, Apr. 2006.

[23] T. Ahonen, A. Hadid, and M. Piettikäinen, "Face description with local binary patterns: application to face recognition," *IEEE Transactions on Pattern Analysis and Machine Intelligence*, vol. 28, no. 12, pp. 2037–2041, Dec. 2006.

[24] D. K. Iakovidis, D. E. Maroulis, and S. A. Karkanis, "An intelligent system for automatic detection of gastrointestinal adenomas in video endoscopy," *Computers in Biology and Medicine*, vol. 36, no. 10, pp. 1084–1103, Oct. 2006.

[25] O. Pujol, D. Rotger, P. Radeva, O. Rodriguez, and J. Mauri, "Near real-time plaque segmentation of IVUS," in *Proceedings of Computers in Cardiology*, Thessaloniki, Greece, 2003, pp. 69–73.

[26] D. Lowe, "Distinctive image features from scale-invariant keypoints," *International Journal of Computer Vision*, vol. 60, no. 2, pp. 91–110, Nov. 2004.

[27] C. Tomasi and T. Kanade, "Detection and tracking of point features," Carnegie Mellon Univ., Pittsburgh, PA, Tech.Rep. CMU-CS-91-132, apr 1991.

[28] J. Shi and C. Tomasi, "Good features to track," in *Proceedings of IEEE Computer Vision and Pattern Recognition Conference*, Seattle, USA, 1994, pp. 593–600.

[29] M. L. Yuan, S. K. Ong, and A. Y. C. Nee, "Registration using natural features for augmented reality systems," *IEEE Transactions on Visualization and Computer Graphics*, vol. 12, no. 4, pp. 569–580, 2006.

[30] M. Slaughter, "Tracking pedestrians with machine vision," *Evaluation Engineering*, vol. 46, no. 2, pp. 56–57, Feb. 2007.

[31] D. Metaxas, G. Tsechpenakis, Z. Li, Y. Huang, and A. Kanaujia, "Dynamically adaptive tracking of gestures and facial expressions," in *Proceedings of 6th International Conference on Computational Science,Part III (Lecture Notes in Computer Science Vol. 3993)*, Reading, UK, 2006, pp. 554–561.

[32] A. Rao, R. K. Srihari, and Z. Zhang, "Spatial color histograms for content-based image retrieval," in *Proceedings of IEEE International Conference on Tools with Artificial Intelligence*, Chicago, USA, 1999, pp. 183–186.

[33] [online], "http://www.bic.mni.mcgill.ca/brainweb/."

[34] J. G. Sled, A. P. Zijdenbos, and A. C. Evans, "A nonparametric method for automatic correction of intensity nonuniformity in mri data," *IEEE Transactions on Medical Imaging*, vol. 17, no. 1, pp. 87–97, Feb. 1998.